Indian Journal of Radio & Space Physics
Vol 41, April 2012, pp 264-270

On the linkage between mesospheric gravity waves and occurrence of equatorial plasma bubble observed during the low solar activity

A Taori[1,$,*], V Kamalakar[2], L M Joshi[1], S Sripathi[3] & A K Patra[1]

[1]National Atmospheric Research Laboratory, Gadanki 517 112, India
[2]Department of Physics, S V University, Tirupati 517 502, India
[3]Indian Institute of Geomagnetism, Panvel, Navi Mumbai 410 218, India
[$]E-mail: alok.taori@gmail.com

Received October 2011; accepted 22 March 2012

In this paper, the linkage between the low-latitude mesospheric gravity waves and the equatorial plasma bubble (EPB) have been investigated using simultaneously Rayleigh lidar and VHF radar observations from Gadanki (13.5°N, 79.2°E) and ionosonde observations from Tirunelveli (8.7°N, 77.8°E) made between 2007 and 2009 when solar activity was undergoing a deep minima. The two sets of observations have been analysed, each comprising of one case having EPB and another without EPB observed on two nearby nights. Observations show that the occurrences of plume structures in the radar observations are found to have a close link with the amplitudes of the short period gravity waves in the mesospheric temperature. It is argued that such waves have an important role in seeding the Rayleigh-Taylor (RT) instability manifesting EPB.

Keywords: Equatorial plasma bubble (EPB), Equatorial spread F (ESF), Mesospheric gravity wave, Rayleigh-Taylor (RT) instability

PACS Nos: *92.60.hc; 94.20.dt*

1 Introduction

Study of equatorial plasma bubble (EPB), which manifests in the form of spread echoes in ionogram (commonly known as equatorial spread F or ESF), plume in radar observations, and depletion in 630 nm airglow intensity measurements, is important not only for studying plasma instability physics and neutral ion coupling but also for their relevance in satellite based communication and navigation systems[1]. As is understood, the Rayleigh-Taylor (RT) instability is the primary governing mechanism manifesting the EPB and the post-sunset pre-reversal enhancement (PRE) in the zonal electric field plays an important role. A quasi-sinusoidal perturbation, however, is required at the bottom of the F-region of the ionosphere for seeding the RT instability due to the slow growth rate of the RT instability. It has been shown that upward propagating gravity waves, tides and planetary waves play an important role in the EPB occurrence[2-6]. As far as the seeding by the gravity waves is concerned, it becomes essential that the gravity wave amplitudes at the mesospheric altitudes should be large to overcome the viscous dissipation so that they can propagate into the ionosphere[7-9]. On the other hand, some of the studies suggest that shear flow at the bottom of the F-region can generate plasma structures providing necessary seed for the excitation of plasma irregularities through the RT instability, indicating that seed perturbation of lower atmospheric origin (i.e. middle atmosphere) is not always necessary[10]. In addition, in the recent years, significant attention has been paid in detecting the large scale wave structures (LSWS) in the F-region and in evaluating its role in seeding EPB[11]. In a more recent study, Narayanan *et al.*[12] argued that while the LSWS may play important role, the importance of the short period gravity waves can not be ignored. Further, in a recent work, based on the simultaneous observations of mesospheric temperature, E-region field-aligned irregularity (FAI) drift velocity, and F-region FAI made from Gadanki (13.5°N, 79.2°E, 6.5°N dip latitude), Taori *et al.*[13] have shown a close correspondence between some of the wave periods observed in mesospheric temperature and E-region FAI drifts. Further, the temporal spacing between F-region FAI structures matched exceeding well with the wave periods in mesospheric temperature and E-region FAI drifts[13]. These observations seem to strengthen the notion that upward propagating gravity waves (as observed in the mesospheric temperature) induced electric fields (as noted in the E-region FAI drifts) when mapped to the

F-region, provide necessary seed perturbation for the growth of the RT instability at the F-region manifesting EPB[14]. As the F-region base height during the low solar activity period is mostly below 300 km over the magnetic equator, a level which is significantly lower than that during the high solar activity[15], observations made from Gadanki provide a unique opportunity to examine the role of gravity waves in seeding the RT instability over the magnetic equator[16].

In this context, simultaneous observations made using the Rayleigh lidar and the MST radar from Gadanki (13.5°N, 79.2°E, 6.5°N dip latitude) and ionosonde observations from Tirunelveli (8.7°N, 77.8°E, 1.1°N dip latitude) during 2007 and 2009 have been analysed to examine the possible linkage between the mesospheric gravity waves and the occurrence of EPB. The two sets of observations have been analysed, each comprising of one case having EPB and another without EPB observed on two nearby nights. These results are presented and discussed in the light of current understanding on the role of gravity waves in generating EPB.

2 Brief description of the experiments and data

Observations presented in this work were made using the MST radar and the lidar located at Gadanki, and an ionosonde located at Tirunelveli. Figure 1 shows a map with geographic and geomagnetic coordinate systems displaying the locations of Gadanki and Tirunelveli. It may be noted that Tirunelveli is located in the close vicinity of the magnetic equator. The two sets of observations have been examined, one set made on 17 February and 20 February 2007 (geomagnetic Ap values are 9 and 2, respectively) and another set made on 21 February and 22 February 2009 (geomagnetic Ap values are 3 and 4, respectively). EPB was observed on 20 February 2007 in the first case and 22 February 2009 in the second case, as evident from the radar maps in the form of plume structures.

2.1 MST radar

The radar observations of F-region FAI were made using the MST radar at Gadanki[17]. This radar is a high power coherent pulsed Doppler radar, operating at 53 MHz with a maximum peak power-aperture product of 3×10^{10} Wm^2. The radar antenna was phased to form the main beam at 14.8° zenith angle due magnetic north so that E and F-region echoes arising from the FAI can be observed. Power spectral data were collected online with height and time resolutions of 2.4 km and 30 s, respectively, which were processed offline to obtain signal-to-noise ratio (SNR), mean Doppler velocity and spectral width.

2.2 Lidar

Temperature observations used here were made using a high power lidar located at Gadanki[18]. The lidar uses a Nd-YAG pulsed laser that provides 0.5 Joule at 532 nm and a receiving telescope of 75 cm diameter. The received signals were sampled at 300 m resolution and photon counts were averaged online for 250 s. The deduced temperature has an accuracy of 0.5–1.5 K in stratospheric altitudes and 2–3 K at mesospheric altitudes[18]. For the present study, similar to the earlier study[13], a 3-point running average has been made in time and 5 km height averaging to smooth out short-term fluctuations and to enhance the data quality at mesospheric altitudes. Further, the temperature variations in the height range of 70-75 km are used in the current study.

2.3 Ionosonde

The ionosonde observations used in the present study were made using a Canadian Advanced Digital Ionosonde (CADI)[19] located at Tirunelveli. The CADI consists of a transmitter, four receivers, and two sets of antenna system. The transmitter antenna is a delta antenna, and the receiver antenna array consists of four dipoles arranged in the form of a square. The

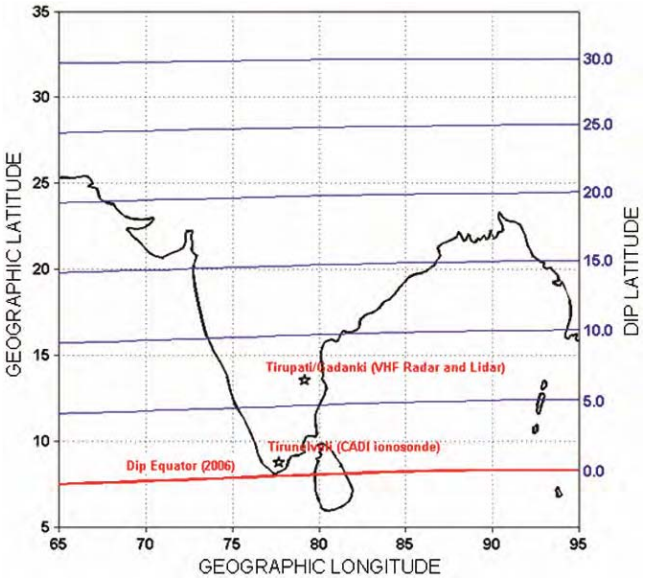

Fig. 1 — Geographic and geomagnetic coordinates of the observational sites used in the present study (shown as star) (red line represents the geomagnetic equator)

transmitter unit is capable of operating in the frequency range of 1-20 MHz with a peak power of 600 W. The pulse length is 40 μs and samples are taken at every 20 μs proving a height resolution of 3 km. Echoes are received at 3 km resolution up to an altitude of 1020 km.

3 Results

VHF radar observations corresponding to the case 1 are shown in Fig. 2. The left panel shows the height-time-SNR map of FAI echoes observed on 17 February 2007 while the right panel depicts that of 20 February 2007. The white spaces represent data gaps due to non-operation of the radar. On 20 February 2007, radar echoes appeared in the form of multiple periodic plumes with large SNR during 2200-0000 hrs IST and in the height region of 200-400 km. These plume structures are known to be associated with the plasma bubbles[1,2]. The plume structures were found to be temporally separated by ~ 0.5 h. On 17 February 2007, however, no such plume structure was observed.

To study the atmospheric waves in the mesospheric temperature, temperature observations made in the height region of 70-75 km have been examined. In order to derive the wave parameters, a simple best-fit analysis has been performed on the time series of temperature variation, which is obtained after subtracting the mean temperature from individual data points, as follows:

$$Y = A_1 Cos[\pi \frac{(t-\phi_1)}{T_1}] + A_2 Cos[\pi \frac{(t-\phi_2)}{T_2}] + A_3 Cos[\pi \frac{(t-\phi_3)}{T_3}] \quad \ldots (1)$$

where, A_1, A_2, and A_3, are the amplitudes; T_1, T_2 and T_3, the half periods; and Φ_1, Φ_2 and Φ_3, the phases at a time, t, of the fitted waves. The choice of wave components is based on the three most significant periods obtained through Lomb-Scargle periodogram analysis. The above best-fit model has been chosen to obtain the wave periodicity, amplitude, and phase because for discrete, unevenly spaced and under-sampled data. Also the best-fit analysis is known to provide better estimates and introduces lesser biases than those of other methods[20].

The top plot in Fig. 3(a), presented as filled circles with connecting lines, shows the temperature deviations (after subtracting the mean temperature) obtained using the lidar observations corresponding to 70-75 km altitudes made on 17 February 2007. Plotted together are the results of the above described best-fit model (center solid lines) together with the 90% confidence levels (solid lines). It may be mentioned that on this night, the mean temperature was 205.4 K. The bottom plot shows individual wave components as described in Eq. (1). It is evident that on this night, temperature variability is dominated by 0.7 ± 0.2 h, 0.5 ± 0.2 h and 1.2 ± 0.3 h wave periods with their corresponding amplitudes of 13 ± 2.3 K, 7 ± 1.4 K and 3 ± 1 K, respectively. Results obtained for the observations made on 20 February 2007 are shown in Fig. 3(b) in the same way as those shown in Fig. 3(a). On this night, the mean temperature was 197.2 K. It is noted that the dominant wave periodicity on this night are 0.42 ± 0.13 h, 10 ± 1.4 h and 0.8 ± 0.2 h with their corresponding amplitudes of 11 ± 1.5 K, 7.5 ± 0.9 K and 6 ± 0.98 K, respectively. It may be mentioned here that the periods utilized in

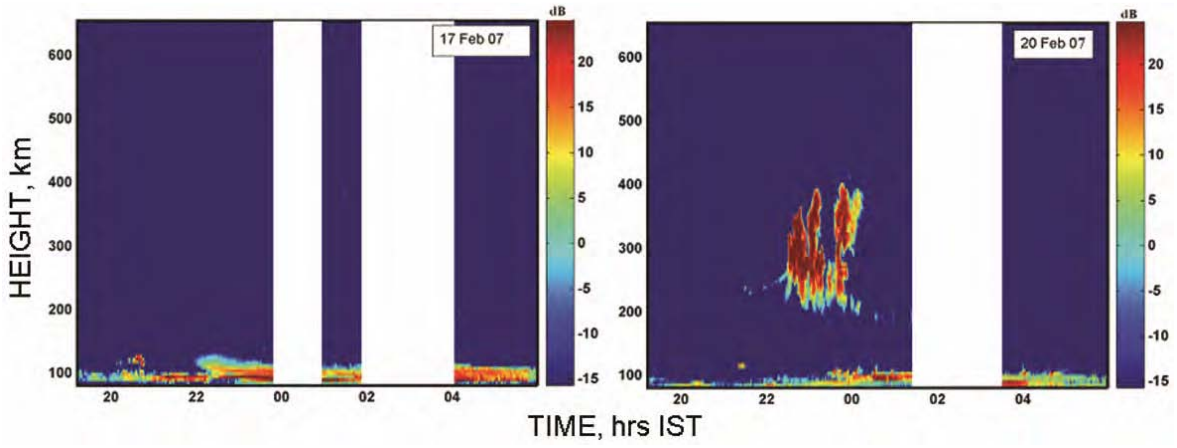

Fig. 2 — Height – time variations of SNR associated with the F-region FAI observed by the Gadanki radar on 17 February 2007 (left panel), and 20 February 2007 (right panel)

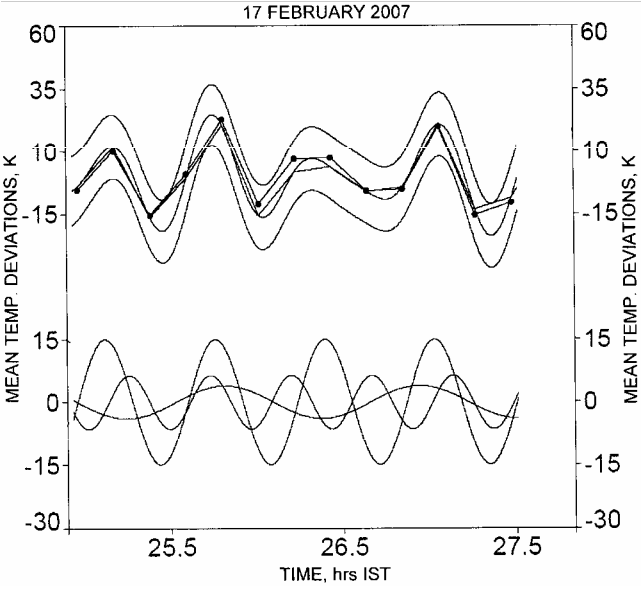

Fig. 3(a) — (top) Mean temperature deviations corresponding to 70-75 km altitudes (filled circles with connecting lines) of 17 February 2007 lidar temperature data (solid lines plot the best-fit results with 90% confidence bands); (bottom) Variation of individual wave component utilized in the best-fit model

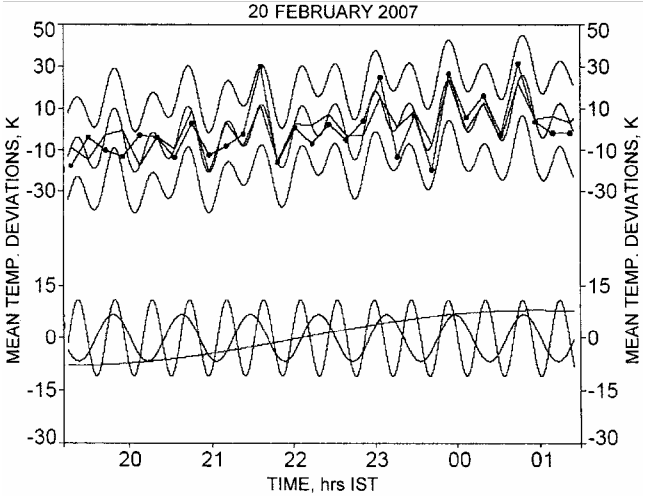

Fig. 3(b) — Height – time variations of SNR associated with the F-region FAI observed by the Gadanki radar on 20 February 2007

the best-fit model are the most significant in the data, which was also verified through periodogram analysis (not presented here). It may also be mentioned that by ignoring one of these dominant periods in the best-fit model, it is found that the χ^2 values significantly deviate from one, implying that best-fit model used for the present analysis is quite reliable for the present purpose.

VHF radar observations corresponding to the case 2 are presented in Fig. 4 in the same way as that of case 1 (Fig. 2). The left and right panels show SNR maps of radar echoes obtained on 21 February and 22 February 2009, respectively. In this case, plasma plume structures were observed on 22 February 2009, but they were confined to a narrow altitude region of 200-300 km unlike those observed on 17 February 2007 (Fig. 2). Despite this difference, one can note the temporal separation between the plumes, which is about 0.4 h. On 21 February 2009, no F-region irregularity structures were observed.

Temperature observations corresponding to these nights (21 and 22 February 2009) were performed in the same way as those for 17 and 20 February 2007 (shown in Fig. 3) and the results are presented in Figs 5(a and b). The mean temperatures were 196.4 K and 196.2 K on 21 February and 22 February 2009, respectively. Figure 5(a) shows the results corresponding to 21 February 2009. On this night, the dominant periods were 0.6 ± 0.05 h, 0.7 ± 0.2 h and 1.9 ± 0.3 h with amplitudes of 5.2 ± 0.8 K, 5 ± 0.6 K and 4.5 ± 0.6 K, respectively. Similar analysis performed on 22 February 2009 data, shown in Fig. 5(b) reveals the presence of waves with periods of 0.4 ± 0.1 h, 6 ± 0.8 h and 0.8 ± 0.17 h and amplitudes of 16 ± 3.2 K, 15 ± 2.3 K and 12 ± 1.4 K, respectively.

It may be important to mention that the vertical wavelength of the short period gravity waves presented in Figs (3 and 5), estimated from the vertical profile of temperature obtained from lidar observations (not shown here), was ~ 35 km. Similar vertical wavelength was also obtained earlier for the short period gravity waves[13].

To investigate the influence of the background ionospheric conditions in the formation of EPB, the base height of the F-layer has been examined. Figure 6 shows the base height of the F-layer for the four cases under consideration. The top panel [Fig. 6(a)] shows the F-layer height movement for first two cases (17 February and 20 February 2007). Solid straight line parallel to horizontal axis in each plot shows the duration of ESF occurrence in ionogram. It is clear that on 20 February 2007, the F-layer reached an altitude of ~310 km before the onset of ESF. This height was substantially larger than the base height of the F-layer observed on 17 February 2007 (~ 260 km at 1800 hrs IST). The base height of the F-layer corresponding to the other two cases, i.e.

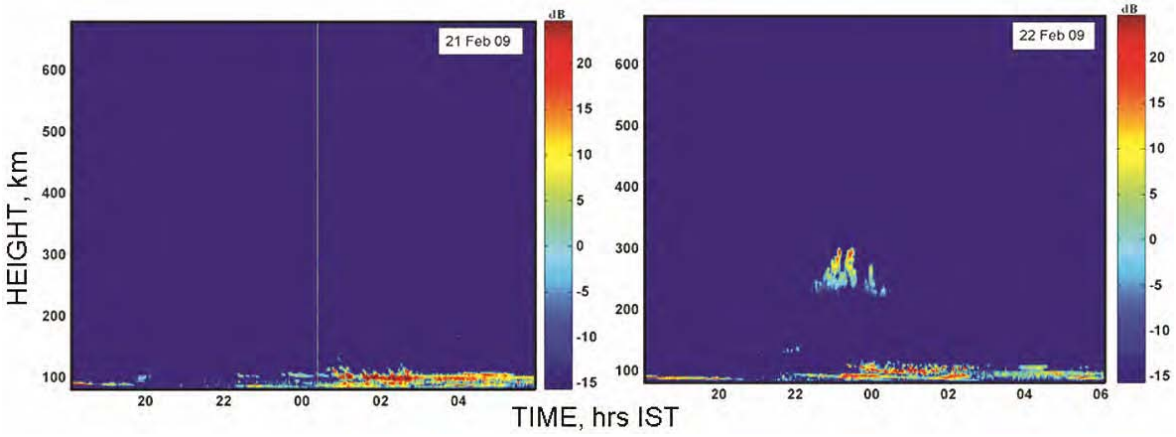

Fig. 4 — Height – time variations of SNR associated with the F-region FAI observed by the Gadanki radar on 21 February 2009 (left panel), and 22 February 2009 (right panel)

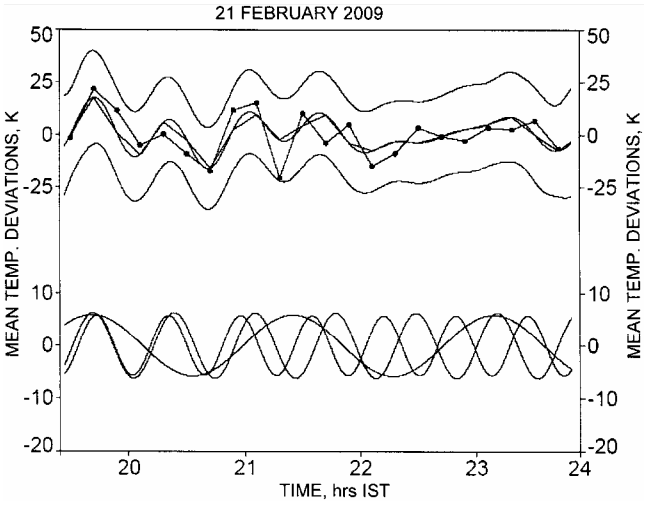

Fig. 5(a) — (top) Mean temperature deviations corresponding to 70-75 km altitudes (filled circles with connecting lines) of 21 February 2009 lidar temperature data (solid lines plot the best-fit results with 90% confidence bands); (bottom) Variation of individual wave component utilized in the best-fit model

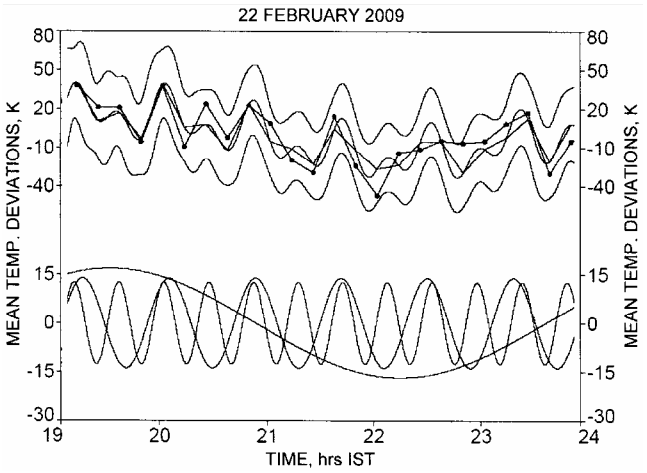

Fig. 5(b) — Height – time variations of SNR associated with the F-region FAI observed by the Gadanki radar on 22 February 2009

21 and 22 February 2009, are shown in Fig. 6(b). It was noted that the base heights on both the nights are nearly the same (~ 275 km). ESF, however, was observed only on 22 February 2009.

4 Discussions

The observational results revealed that EPB/ESF was observed when h'F was ≥ 275 km and the amplitudes of mesospheric gravity waves with wave period of ~0.5 h were in the range of 11-16 K. The observations also revealed that despite the fact that wave amplitude of 0.8 h was 13 K on 17 February 2007, no EPB/ESF was observed when h'F was 260 km. Importantly, on the two nights when EPB/ESF was observed, the temporal spacings of the plumes and the gravity wave periods with large amplitude (11-16 K) agreed extremely well. This finding is in agreement with earlier suggestion that gravity waves amplitude and generation of EPB may be closely related[3,4,7]. While the present observations indicate the possible role of gravity waves in seeding EPB/ESF on the two nights, the height of the F-layer possibly decides the pre-requisite condition whether the seeding in question would eventually manifest in EPB/ESF or not[21]. One issue that remains to be addressed is the true linkage between the mesospheric gravity waves and the seed perturbations at the bottom of the F-region.

As far as the role of mesospheric gravity waves in the EPB phenomenon is concerned, it is essential that they should reach the base of the F-layer where the seeding for the RT instability takes place. This implies that the gravity wave, in question, should

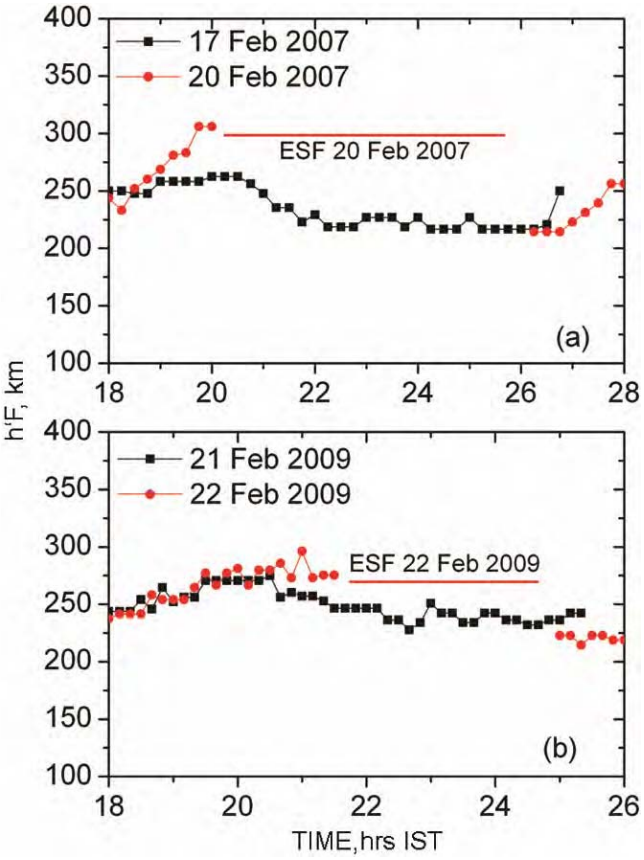

Fig. 6 — Variation in the base height of F-layer for the February 2007 cases (top panel) and February 2009 cases (bottom panel) (straight lines parallel to x-axis show the time of ESF occurrence in ionosonde data)

have large enough vertical wavelength and they should not undergo viscous dissipation in order to maintain their amplitudes. The vertical wavelength inferred for the short period waves was about 35 km, which does not appear to be adequate to reach the F-region un-attenuated. Assuming that there were genuine difficulties for these waves to propagate directly to the F-region (although there is no experimental evidence), there lies another way through which these waves would still be effective in the EPB formation process. The alternate way, which is believed to be the case here, is the propagation of these waves to the E-region and manifesting there in the form of polarization electric field[13,14,16,22]. Considering that the present observations were made from Gadanki, a location of low magnetic latitude (6.5°N), the potential of mapping of such polarization electric fields along the magnetic field lines up to the equatorial F-region and seeding the RT instability is quite promising[13,16]. It may be recalled that the gravity wave period under consideration is about 0.5 h and for the vertical wavelength of 35 km, the horizontal wavelength can be estimated using the linear dispersion relation. For the above wave parameters, the horizontal wavelength is estimated to be 175 km. Now, assuming that the polarization electric field associated with such gravity waves in the E-region have the same horizontal wavelength, it is very likely that such electric field can map without much attenuation to the equatorial F-region. Also, the horizontal wavelength of 175 km is very much suitable for seeding the RT instability leading to the formation of EPB. In an earlier study[13], a close correspondence has been found between the mesospheric gravity waves and the E-region FAI velocity perturbations, supporting the notion that the gravity waves could induce electric field in the E-region. In this context, it may be worth considering the temporal spacing of the plume structures observed by the radar. As mentioned earlier, the temporal spacing of the plumes was also about 0.5 h. Assuming that the background zonal plasma drift is ~100 m s^{-1}, one can roughly estimate the spatial spacing of the plumes (representing bubbles) to be 180 km, which is very much consistent with the horizontal wavelength of the gravity waves observed at the mesospheric height.

Having said that gravity waves could potentially seed the RT instability for the generation of EPB, it is important to examine the role of the F-layer base height in the growth rate of the instability ($\gamma = \frac{1}{n}\frac{\partial n}{\partial h}\frac{g}{\nu_{in}}$, where, n, is the background electron density; g, the acceleration due to gravity; and ν_{in}, the neutral-ion collision frequency; and $\partial n/\partial h$, the electron density gradient). As far as the role of the F-layer base height is concerned, it comes in the form of ν_{in} in the growth rate. Since ν_{in} decreases with solar activity and the observations presented here correspond to the solar minimum (i.e. during 2007 and 2009), the RT instability growth rate is expected to be positive even for low h'F (Ref. 15). Furthermore, low peak electron density prevailing during the low solar condition would also help the growth rate of the RT instability. Manju *et al.*[15], using ionosonde observations from Trivandrum, showed that the threshold height of h'F for the ESF to occur is 225 km during the low solar activity. The observed h'F values in the present study, however, were more

than 225 km in all the cases. In fact, Abdu *et al.*[21] clearly presented cases when h'F reached beyond 400 km, but there were no ESF. This underlines the need of seeding for the RT instability to grow. The present study, although is based on limited observations, suggests that the gravity wave seeding in question is no more a simple one. It may also be possible that the large-scale wave structure (LSWS) help in making the background condition conducive for the effective seeding by the gravity waves. Further investigation, based on a larger database than the one used here, would be required to bring out the relative roles of gravity waves and LSWS in the formation of EPB.

Acknowledgements

The authors gratefully acknowledge the MST radar and Rayleigh lidar staff for making the observations utilized in this study. The geomagnetic Ap values were taken from http://wdc.kugi.kyoto-u.ac.jp/wdc/Sec3.html.

References

1 Hysell D L, Kelley M C, Swartz W E, Farley D T & Woodman R F, Seeding and layering of equatorial spread F by gravity waves, *J Geophys Res (USA)*, 95 (1990) pp 17253–17260.

2 Kelley M C, Larsen M F, LaHoz C A & McClure J P, Gravity wave initiation of equatorial spread F: A case study, *J Geophys Res (USA)*, 86 (1981) pp 9087–9100.

3 Taylor M J, Pautet P-D, Medeiros A F, Buriti R, Fechine J, Fritts D C, Vadas S L, Takahashi H & Sao Sabbas F T, Characteristics of mesospheric gravity waves near the magnetic equator, Brazil, during the SpreadFEx campaign, *Ann Geophys (Germany),* 27 (2009) pp 461–472.

4 Takahashi H, Taylor M J, Pautet P-D, Medeiros A F, Gobbi D, Wrasse C M, Fechine J, Abdu M A, Batista I S, de Paula E R, Sobral J H A, Aruda D & Fritts D C, Simultaneous observation of ionospheric plasma bubbles and mesospheric gravity waves during the SpreadFEx campaign, *Ann Geophys (Germany),* 27 (2009) pp 1477-1487.

5 Fritts D C, Vadas S L, Riggin D M, Abdu M A, Batista I S, Takahashi H, Medeiros A, Kamalabadi F, Liu H L, Fejer B G & Taylor M J, Gravity wave and tidal influences on equatorial spread F based on observations during the Spread F Experiment (SpreadFEx), *Ann Geophys (Germany)*, 26 (2008) pp 3235–3252.

6 Bertoni F C B, Sahai Y, Raulin J-P, Fagundes P R, Pillat V G, Gimenez de Castro C G & Lima W L C, Equatorial spread-F occurrence observed at two near equatorial stations in the Brazilian sector and its occurrence modulated by planetary waves, *J Atmos Sol-Terr Phys (UK),* 73 (2011) pp 457-463, doi: 10.1016/j.jastp.2010.10.017.

7 Taori A, Makela J J & Taylor M, Mesospheric wave signatures and equatorial plasma bubbles: A case study, *J Geophys Res (USA)*, 115 (2010), doi: 10.1029/2009JA015088.

8 Taori A, Dashora N, Raghunath K, Rusell III J M & Mlynczak M G, Simultaneous mesosphere, thermosphere-ionosphere parameter measurements over Gadanki (13.5°N, 79.2°E) - first results, *J Geophys Res (USA)*, 116 (2011), doi: 10.1029/2010JA016154.

9 Vadas S L, Horizontal and vertical propagation and dissipation of gravity waves in the thermosphere from lower atmospheric and thermospheric sources, *J Geophys Res (USA),* 112 (2007) A06305, doi: 10.1029/2006JA011845.

10 Kudeki E, Akgiray A, Milla M, Chau J L & Hysell D L, Equatorial spread–F initiation: Post-sunset vortex, thermospheric winds, gravity waves, *J Atmos Sol-Terr Phys (UK)*, 69 (2007) pp 2416 – 2427.

11 Tsunoda R T, Satellite traces: An ionogram signature for large-scale wave structure and a precursor for equatorial spread F, *Geophys Res Lett (USA),* 35 (2008) L20110, doi: 10.1029/2008GL035706.

12 Narayanan V L, Taori A, Patra A K, Emperumal K & Gurubaran S, On the importance of wave-like structures in the occurrence of equatorial plasma bubbles: A case study, *J Geophys Res (USA)*, 117 (2012) A01306, doi: 10.1029/2011JA017054.

13 Taori A, Patra A K & Joshi L M, Gravity wave seeding of equatorial plasma bubbles: an investigation with simultaneous F-region, E-region and middle atmospheric measurements, *J Geophys Res (USA)*, 116 (2011), doi: 10.1029/2010JA016229.

14 Prakash S, Production of electric field perturbations by gravity wave winds in the E region suitable for initiating equatorial spread-F, *J Geophys Res (USA)*, 104 (1999) pp 10051–10069.

15 Manju G, Devasia C V & Sridharan R, On the seasonal variations of the threshold height for the occurrence of equatorial spread-F during solar minimum and maximum years, *Ann Geophys (Germany),* 25 (2007) pp 855-861.

16 Patra A K, Some aspects of electrostatic coupling between E and F-regions relevant to plasma irregularities: A review based on recent observations, *J Atmos Sol-Terr Phys (UK),* 70 (2008) pp 2159 – 2171.

17 Rao P B, Jain A R, Kishore P, Balamuralidhar P, Damle S H & Vishwanathan G, Indian MST radar 1: System description and sample vector wind measurements in ST mode, *Radio Sci (USA)*, 30 (1995) pp 1125-1138.

18 Sivakumar V, Rao P B & Krishnaiah M, Lidar studies of stratosphere and mesosphere thermal structure over a low latitude: Comparison with satellite and models, *J Geophys Res (USA)*, 108 (2003) 4342, doi: 10.1029/ 2002JD003029.

19 Grant I F, MacDougall J W, Ruohoniemi J M, Bristow W A, Sofko G J, Koehler J A, Danskin D & Andre D, Comparison of plasma flow velocities determined by the ionosonde Doppler drift technique, SuperDARN radars, and patch motion, *Radio Sci (USA),* 30 (1995) pp 1537–1549.

20 von Clarmann T, Stiller G, Grabowski U, Eckert E & Orphal J, Technical note: Trend estimation from irregularly sampled, correlated data, *Atmos Chem Phys (Germany)*, 10 (2010) pp 6737 -6747, doi: 10.519/acp-10-6737-2010.

21 Abdu M A, de Mediros R T, Bittencourt J A &. Batista I S, Vertical ionization drift velocities and range type spread F in the evening equatorial ionosphere, *J Geophys Res (USA),* 88 (1983) pp 399-402.

22 Varney R H, Kelley M C & Kudeki E, Observations of electric fields associated with internal gravity waves, *J Geophys Res (USA)*, 114 (2009) A02304, doi: 10.1029/2008JA013733.